# NASA TECHNICAL NOTE

NASA TN D-7908 e.1

NASA TN D-7908

# RADIATED NOISE FROM
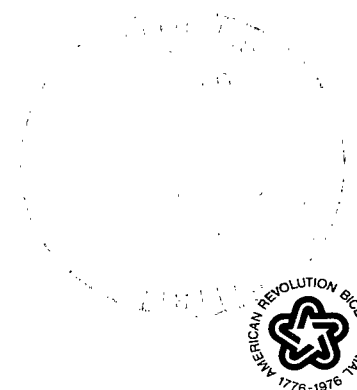# AN EXTERNALLY BLOWN FLAP

*N. N. Reddy*

  *Langley Research Center*

*J. C. Yu*

  *The George Washington University*
  *Joint Institute for Acoustics and Flight Sciences*

*Langley Research Center*
*Hampton, Va. 23665*

NATIONAL AERONAUTICS AND SPACE ADMINISTRATION • WASHINGTON, D. C. • JULY 1975

| 1. Report No. NASA TN D-7908 | 2. Government Accession No. | 3. Recipient's Catalog No. |
|---|---|---|
| 4. Title and Subtitle RADIATED NOISE FROM AN EXTERNALLY BLOWN FLAP | | 5. Report Date July 1975 |
| | | 6. Performing Organization Code |
| 7. Author(s) N. N. Reddy and J. C. Yu | | 8. Performing Organization Report No. L-9895 |
| 9. Performing Organization Name and Address NASA Langley Research Center Hampton, Va. 23665 | | 10. Work Unit No. 505-03-11-03 |
| | | 11. Contract or Grant No. |
| 12. Sponsoring Agency Name and Address National Aeronautics and Space Administration Washington, D.C. 20546 | | 13. Type of Report and Period Covered Technical Note |
| | | 14. Sponsoring Agency Code |

15. Supplementary Notes

J. C. Yu is an assistant research professor, The George Washington University, Joint Institute for Acoustics and Flight Sciences.

16. Abstract

The far-field noise from subsonic jet impingement on a wing-flap with a $45^{\circ}$ bend has been experimentally investigated. The test parameters are jet Mach number and flap length. For long flaps, the primary source mechanisms are found to be turbulent mixing and flow impingement. For short flaps, the interaction of turbulent flow with the flap trailing edge appears to strongly influence the radiated noise.

| 17. Key Words (Suggested by Author(s)) Externally blown flap Noise radiation Aerodynamic noise Flow-surface interaction noise | 18. Distribution Statement Unclassified — Unlimited New Subject Category 71 | | |
|---|---|---|---|
| 19. Security Classif. (of this report) Unclassified | 20. Security Classif. (of this page) Unclassified | 21. No. of Pages 36 | 22. Price* $3.75 |

# RADIATED NOISE FROM AN EXTERNALLY BLOWN FLAP

N. N. Reddy[*]
Langley Research Center

J. C. Yu
Joint Institute for Acoustics and Flight Sciences
George Washington University

## SUMMARY

The results of an experimental investigation of the noise radiated from a subsonic air jet impinging on wing-flap with a $45^O$ bend are presented. From the total radiated acoustic power, directivity pattern, and power spectra, an attempt was made to separate the various possible noise source mechanisms contributing to the total noise of a blown flap. The test parameters are jet Mach number and flap length. The results indicate that for long flaps (for which the flow velocity leaving the trailing edge is small), the total radiated acoustic power depends on the jet velocity raised to the eighth power, and the acoustic power is increased by about 5 dB by introduction of the wing-flap into the jet flow. Therefore, for this configuration, the primary noise-generation source mechanisms are attributed to turbulent mixing of the jet flow modified by the rigid surface, and to impingement of the turbulent flow on the rigid surface. For short flaps, the acoustic power depends on the jet velocity raised to between the fourth and fifth power, depending on the trailing-edge location with respect to the jet exhaust. The noise-generation mechanism for short flaps is more complex. Turbulence flow interacting with the edge appears to strongly influence the radiated noise.

## INTRODUCTION

Short take-off and landing (STOL) aircraft should be able to operate in proximity to residential and commercial areas. This requirement imposes important operational and environmental criteria. The angles of climbout from and approach to the airport must be steeper for STOL aircraft than for conventional take-off and landing (CTOL) aircraft. Therefore, the integrated lift propulsion system for a STOL vehicle should provide more lift and a higher thrust-to-weight ratio to permit a shorter runway. The primary environmental criteria are stringent community noise restrictions. The

---

[*]NRC-NASA Resident Research Associate, now with Lockheed-Georgia Co., Marietta, Georgia.

special problem for STOL aircraft is that the requirements for ground noise exposure (noise footprint) are more restrictive than for CTOL aircraft (ref. 1), whereas the operational requirements are more demanding.

The blown flap is one of the proposed concepts for integrated power plants of STOL aircraft. The lift augmentation from this method is obtained by deflecting the engine exhaust downward by means of a wing with auxiliary flaps. Two configurations are under consideration for STOL aircraft, the externally blown flap and the upper surface blown flap. Previous STOL noise studies by NASA and other organizations have emphasized the definition of the radiation field for various STOL configurations. The far-field noise studies bear out certain important scaling laws that are needed to extrapolate small-scale model data to the radiated noise for full-scale aircraft. These investigations have also been helpful in providing preliminary guidelines for aircraft designers to assess the trade-off between the noise and performance. These studies establish that the blown flap generates considerably more noise than does free jet mixing (refs. 1 to 4). To devise any viable noise reduction technique requires an understanding of the blown-flap noise generation and propagation mechanism.

The physical mechanisms for the additional noise generation in blown flaps are not yet completely understood. However, the experimental results available in the literature suggest three possible mechanisms for the additional noise production: flow impingement on the surface, wall turbulent boundary layer (wall jet), and edge noise. The edge noise is the noise generated in the vicinity of the trailing edge by the fluctuating forces and/or the fluctuating stresses and diffracted by the edge. The physical configuration of a realistic externally blown flap is very complex. At present, no viable theoretical analysis exists to account for the sound generation from an externally blown flap. Some limited theoretical studies relevant to blown-flap noise generation are reviewed in the appendix, but these studies were made for highly idealized models. Most previous experimental investigations were conducted on externally blown flaps which had complicated geometry, and it is difficult to identify the various noise sources from the test results. To bridge the gap between the theoretical and experimental investigations and to separate possible source mechanisms contributing to the total noise of a blown flap, work should begin with a simple but realistic experimental configuration.

This report presents some experimental results of the acoustic power, directivity, and power spectrum of a subsonic air jet impinging on a wing-flap configuration with a 45$^{\circ}$ bend. The slots which normally would exist in the wing-flap were eliminated to simplify the geometry. The test parameters are jet Mach number and flap length.

## SYMBOLS

| | |
|---|---|
| $c_o$ | ambient speed of sound |
| $d$ | diameter of nozzle |
| $f$ | frequency |
| $f_p$ | spectral peak frequency |
| $I_d$ | intensity of sound generated by dipoles |
| $I_q$ | intensity of sound generated by quadrupoles |
| $l_f$ | length of flat part of flap trailing-edge section after $45^o$ bend |
| $M_j$ | jet Mach number, $V_j/c_o$ |
| $R$ | distance between nozzle exit and microphone |
| $U_o$ | typical mean velocity |
| $V_j$ | jet exit velocity |
| $X,Y,Z$ | axes used to define flap position |
| $x,y,z$ | coordinates along $X$, $Y$, and $Z$ axes, respectively |
| $\delta$ | boundary-layer thickness |
| $\theta$ | azimuthal angle |
| $\rho_o$ | density of air |
| $\phi$ | circumferential angle |

Abbreviations:

| | |
|---|---|
| PWL | acoustic power level, dB (re 0.1 pW) |
| $PWL_t$ | total acoustic power level, dB (re 0.1 pW) |
| OASPL | overall sound pressure level, dB (re 20 $\mu N/m^2$) |
| SPL | sound pressure level, dB (re 20 $\mu N/m^2$) |

3

## APPARATUS AND INSTRUMENTATION

### Blown-Flap Configuration

The wing-flap configuration used in this investigation consisted of two flat plates joined by a curved plate with a 40.6-cm (16-in.) radius of curvature as shown in figure 1. The slots normally present in the wing-flap were eliminated. The spanwise dimension of the flap was 61.0 cm (24 in.).

The flap lengths were varied by changing the flat part of the trailing-edge section to the required size. Four flap trailing-edge lengths, 3.8 cm (1.5 in.), 19.1 cm (7.5 in.), 64.8 cm (25.5 in.), and 121.9 cm (48 in.), were used in these experiments.

The components of the flap were machined from 2.5-cm-thick (1-in.) aluminum plate. Aluminum channel reinforcement was used in the curved part of the flap to ensure the rigidity of the entire wing-flap assembly. A contoured converging circular nozzle with a 5.1-cm (2-in.) exit diameter and a contraction ratio of 16 was used to generate the impinging flow.

### Anechoic Chamber and Flow System

The anechoic chamber in which free-field acoustic data were taken has a design cutoff frequency of 100 Hz. The dimensions of the chamber were 7.6 m (25 ft) by 7.6 m (25 ft) by 7.0 m (23 ft), measured from wedge tip to wedge tip. A detailed description of the chamber construction and performance is available in reference 5. The chamber was calibrated for its free-field characteristics during the present investigation, and the anechoic room had satisfactory free-field characteristics down to 100 Hz.

The air supply system has the capability of producing a continuous jet flow from a 5.1-cm (2-in.) nozzle at a maximum stagnation pressure of 2.07 MN/m$^2$ (300 psig) and at room temperature. The air flow is controlled by a system of pressure controllers located in a room adjacent to the anechoic chamber. The stagnation pressure could be maintained within 2 percent of the predetermined value.

### Reverberation Room and Blowdown Jet Facility

The Langley 55-foot vacuum cylinder shown schematically in figure 2, was used as a blowdown jet facility and as a reverberation chamber to measure the radiated sound power. The volume of the chamber is 2830 m$^3$ (10$^5$ ft$^3$), and it is possible to achieve a vacuum inside the cylinder down to 10$^{-4}$ torr. The pressure inside the chamber is monitored by a vacuum gage with an accuracy of 133 N/m$^2$ (1 mm Hg). A 1.1-m-long (3.5-ft) transition section converging from 30.5 cm (12 in.) to 20.3 cm (8 in.) was mounted on one of the 30.5-cm (12-in.) ports on the chamber wall. The nozzle was mounted on the converging end of the transition, so that the exit of the nozzle was about 1.4 m (4.5 ft) from

the chamber wall. (See fig. 2.) A bellmouth inlet connected to the port from outside the cylinder wall induced the smooth flow from atmosphere (high pressure) to the chamber (low pressure) through the nozzle. A pneumatically controlled quick-release valve installed at the inlet of the port was used to start the jet flow. The rate of pressure equalization in the chamber during blowdown was about 11.1 $N/m^2$-sec (5 mm Hg/min) at low vacuum. The reverberation chamber was calibrated by taking the average value of several measured reverberation times in 1/3-octave bands with center frequencies varied from 100 Hz to 10 kHz and extrapolated up to 20 kHz. At normal ambient conditions, the reverberation time was about 10 sec for the 100-Hz band and was reduced to 0.6 sec for the 10-kHz band. The reverberation times at selected reduced ambient pressures were also obtained; it was found that the reverberation was independent of chamber pressure.

## EXPERIMENTAL PROCEDURES

The primary experimental variable in this study was the length of the flap $l_f$ defined as the extent of the flap section after the $45^O$ bend (fig. 1). In the total acoustic power and power spectrum measurements, jet exit Mach number was varied from 0.3 to 0.95 and four values of $l_f/d$ (0.75, 3.75, 12.75, and 24.0) were used in attempting to separate the effects of trailing-edge flow, wall jet flow, and impinging flow on noise generation. In the directivity and sound pressure spectrum measurements, two jet exit Mach numbers, 0.49 and 0.84, were used with the flap length held constant at $l_f/d = 3.75$. The distance between the nozzle exit and the flap surface measured along the axis of the jet was chosen at $x/d = 5.75$ so that the impinging region was just downstream of the potential core of the free jet. The nozzle axis was made parallel to the wing-flap surface at $y/d = 2.0$.

### Reverberation Room Measurements

Acoustic measurements in the reverberation room were made with three spatial microphones about 4.6 m (15 ft) away from the wall and about 2.4 m (8 ft) above the removable floor grating. The three microphones were calibrated with a sound-level calibrator at frequent intervals. After closing the doors and sealing the ports and openings, the pressure in the cylinder was reduced to the predetermined value. The quick-release valve was then opened to induce flow through the nozzle to form a jet. The sound pressure levels from the three microphones were averaged electronically, and 1/3-octave-band spectra were obtained on-line with a microphone amplifier, a 1/3-octave filter set, and a graphic level recorder. A block diagram of the instrumentation is shown in figure 3. The frequency range of the analysis was from 100 Hz to 20 kHz. The average of the data from the three microphones was used to compute the acoustic power. However,

it should be noted that the SPL measurements at three spatial locations differed only by about 1 dB from one another. The average value of SPL at each 1/3-octave band and the experimentally determined reverberation time were used in Sabine's formula to compute the spectral distribution of sound power.

## Free-Field Measurements

The directivity of the radiated noise of the simulated externally blown flap was measured in the Langley anechoic noise facility. The geometry of the configuration is symmetrical about only the plane which passes through the jet axis and is perpendicular to the flap surface. Consequently, the directivity was determined from sound measurements taken at a large number of locations distributed over a hemisphere enclosing the source. A single 1.3-cm (0.5-in.) free-field microphone system was used. The microphone was mounted on a 3.1-m-radius (10-ft) boom which could be rotated in two degrees of freedom from the control room. Figure 4 is a photograph showing the experimental model and the microphone boom installed in the anechoic chamber. The microphone was calibrated with a sound-level calibrator. For each test, the stagnation pressure in the nozzle settling chamber was stabilized at the predetermined value. Acoustic data from the microphone were analyzed on-line with a real-time analyzer to obtain 1/3-octave sound pressure spectra from 100 Hz to 40 kHz. The data also were recorded on magnetic tape for further analysis and verification. (See fig. 3 for the block diagram of data acquisition and reduction.) The position of the microphone was changed by remote control on the semispherical surface enclosing the blown-flap configuration with the center of jet exit as origin. The coordinate system for presenting the data is shown in figure 5. This procedure was repeated for several jet velocities and flap lengths.

## RESULTS AND DISCUSSION

The results are presented in the form of total acoustic power, power spectra, overall sound directivity, and sound pressure level spectra; they are discussed in two categories, (1) jet mixing noise and (2) blown-flap noise. In addition to establishing the basic noise characteristics of jet mixing, the results for jet mixing noise are helpful in evaluating the credibility of the acoustic measurements made in the reverberant and free-field environments. Results for blown-flap noise indicate the effect of jet Mach number and flap length on radiated noise and the relative importance of flow impingement and trailing-edge noise.

### Jet Mixing Noise

The total acoustic power and power spectra of jet mixing noise for a 5.1-cm-diameter (2-in.) circular jet were measured in a reverberant chamber over a range of

subsonic Mach numbers. A variation of total radiated acoustic power with jet Mach number is presented in figure 6. These results are compared with earlier free-field measurements made outdoors by the second author using a similar nozzle at the Langley Research Center and with the experimental data obtained by Gruschka and Schrecker (ref. 6) in a reverberant environment. The total radiated acoustic power depends on the eighth power of jet exit velocity and compares well with the data of reference 6. Whereas the total acoustic power computed from the outdoor free-field measurements varies as the eighth power of jet exit velocity, the absolute values are about 5 dB lower than the reverberation room measurements. It is suspected that this apparent discrepancy is due to the difference in the two measurement environments and in the procedures used to compute the total power from free-field measurements. Figure 7 shows the variation of sound pressure level spectra with angle from the forward axis of the jet, and the variation of acoustic power spectra for jet Mach number of 0.85. As expected for jet noise, the peak frequency in the sound pressure level spectra increases as this angle decreases. The power spectral peak is at about 1 kHz, which corresponds to a Strouhal number of about 0.19. These results indicate that the facilities (reverberation chamber and anechoic room) are free from upstream effects and other undesirable noise sources.

### Blown-Flap Noise

Acoustic power and power spectra.- The radiated acoustic power, measured in the reverberant environment, of the jet alone and of the blown-flap configuration for four flap lengths is shown in figure 8 over a range of subsonic jet Mach numbers. The geometrical impingement location (defined as the point of intersection of the jet axis and the wing-flap surface) is slightly downstream of the potential core of the free jet (without the presence of wing-flap). The "impingement-only noise" for circular jet impingement on a large flat board normal to the jet axis (taken from ref. 2) is also included in this figure. The impingement-only noise is defined as the difference between the radiated noise of a jet impinging on a large flat board and the noise of the free jet (without the rigid surface). The nozzle diameter and impingement distance in reference 2 are 5.2 cm (2.05 in.) and 37 cm (14.45 in.), respectively.

The radiated acoustic power dependence of the blown-flap configuration on jet Mach number varies with different flap lengths; as the flap length decreases, the exponent of the velocity decreases (fig. 8). For $l_f/d$ = 12.75 and 24, the jet velocity dependence and the total acoustic power are the same; they vary as $V_j^8$, similar to jet mixing noise. However, the total acoustic power is increased by about 5 dB over the free jet mixing noise. Strong et al. (ref. 7) and Westley et al. (ref. 8) have shown that jet impingement on a rigid surface produces intense surface pressure fluctuations within the stagnation region. For a long flap, edge noise does not contribute significantly to the total noise, since the flow velocity leaving the trailing edge is small. The observed $V_j^8$ dependence

of the total radiated power for the long flap implies that the dipole radiation from surface pressure fluctuations is quite ineffective for jet impingement in spite of the induced high pressure fluctuations. The experimental observation of the total radiated acoustic power variation with jet velocity for long flaps from this study and the impingement-only noise reported in reference 2 seem to confirm the theoretical findings on the dominant noise source mechanism reported by Curle (ref. 9), Phillips (ref. 10), Powell (refs. 11 and 12), and Meecham (ref. 13). When the curvature of the surface is small and the extent of the flap surface is large in comparison with the dominant wavelength of radiated sound, the main source mechanism is of quadrupole nature (because of the fluctuating Reynolds stresses) as evidenced by the observed $V_j^8$ trend.

In figure 8, the acoustic power increases as the flap length decreases at low jet Mach numbers and follows $V_j^5$ and $V_j^4$ for the short flaps. As the jet Mach number increases, the difference in the total acoustic power of the different flap lengths decreases, and the acoustic power converges to nearly the same level near the sonic velocity of the jet. The change in the exponent of the jet exit velocity indicates that the possible noise-generation mechanisms have changed in character because of the presence of the trailing edge in the flow. Ffowcs Williams and Hall (ref. 14) derived the fifth-power velocity dependence of the total radiated acoustic power for an idealized quadrupole source in the vicinity of the scattering edge of a semi-infinite rigid surface. Hayden (ref. 15) obtained sixth-power velocity dependence for the total radiated sound by assuming a line dipole source near the trailing edge. These theoretical predictions appear to be relevant to the sound field observed for the flap length $l_f/d = 3.75$. Since the observed total acoustic power for $l_f/d = 3.75$ depends on $V_j^5$, it is believed that the noise mechanism in this case is closely related to the interaction between the flow turbulence and the trailing edge. It is not possible, however, to determine from the present experimental investigations whether the observed $V_j^5$ dependence is a local phenomenon, as postulated in references 14 and 15, or a global phenomenum involving the entire impinging flow field.

What is more interesting is the observed $V_j^4$ dependence for a very short flap $\left(l_f/d = 0.75\right)$ which indicates the existence of a monopole-type source. The possibility of sound radiation from flap vibration caused by the impinging flow was ruled out because of the massiveness of the flap model. Theoretical developments considering the possible existence of a monopole noise source in flow interacting with a rigid surface are not available. The physical origin of this type of noise-generation mechanism is not clear at this time. However, the $V_j^4$ dependence for the short flap could be a possible guideline for future analytical work. The postulation of a source mechanism model should take into consideration the transition of the source from quadrupole to monopole as the flap length of the externally blown flap is reduced.

8

The power spectra for three flap lengths $\left(l_f/d = 12.75,\ 3.75,\ \text{and}\ 0.75\right)$ are compared in figure 9 for jet Mach numbers of 0.42 and 0.83. Since the noise characteristics for $l_f/d = 24$ are the same as those for $l_f/d = 12.75$, only the results for $l_f/d = 12.75$ are considered in the remaining discussions of this report.

The experimentally obtained 1/3-octave-band power spectra were divided by individual bandwidth to yield the power spectra given in figure 9(a) for $M_j = 0.42$. Since the total acoustic power for the different flap lengths varied very little at higher jet Mach numbers, the power spectral data are normalized, so that the spectral distribution of the radiated sound may be delineated for different flap lengths. The normalization is carried out by dividing the power spectrum by the total power given in figure 9(b) for $M_j = 0.83$. In both figures either the power spectrum or the normalized power spectrum of the jet mixing noise is given for comparisons.

At the low jet Mach number of 0.42 (fig. 9(a)), the power spectra obtained at different flap lengths indicate that the noise radiation from the blown flap is mainly broadband. The increase in noise radiation, as a result of the introduction of the wing-flap into the jet flow, occurs primarily in the low to intermediate frequencies for the short flaps. For the long flap, this increase is relatively small. At high frequencies, above 4 kHz, the increase in noise radiation is also small and the spectral variation is similar to that of jet mixing noise for all test flap lengths. For $l_f/d = 0.75$ and 3.75, the power spectrum is characterized by a single peak; for $l_f/d = 12.75$, however, double peaks are noted in the power spectrum. The lower peak occurs at a very low frequency, around 125 Hz, whereas the second, higher peak nearly coincides with the peak for jet mixing noise. Attempts were made to scale the power spectra by using the flap length and jet exit velocity as scaling parameters, but the data failed to collapse into a single curve. The spectral peak frequency $f_p$ varied with the flap length, but no consistent trend existed. The nondimensionalized spectral peak frequencies $f_p l_f/V_j$ were 0.64, 0.60, and 0.21 for $l_f/d = 0.75,\ 3.75,\ \text{and}\ 12.75$, respectively.

At the high jet Mach number of 0.83 (fig. 9(b)), the shapes of the power spectra above 2 kHz for the three flap lengths are grossly similar to each other and are all similar to the spectrum for jet mixing noise. Below 2 kHz, variation exists among the power spectra for different flap lengths, and this variation becomes more noticeable at lower frequencies. The spectral peak frequencies for the three flap lengths are nearly the same and occur at $f_p d/V_j \approx 0.27$.

The dependence of power spectrum on jet Mach number for a fixed flap length $l_f/d = 3.75$ is illustrated in figure 10. These results reveal that there is a gross similarity in power spectra. The spectral peak frequency is given by $f_p d/V_j \approx 0.15$. The slopes of the spectra are 6 dB per octave in the low-frequency range and between –6 and

-9 dB per octave in the high-frequency range. A substantial increase in low-frequency spectral contents occurs as the jet Mach number is reduced.

Directivity pattern.- The directivity pattern of sound generated by the blown flap was determined for three flap lengths at jet Mach numbers of 0.49 and 0.84. These results were similar for a given flap length, except that the levels of OASPL at corresponding angular positions were higher at higher Mach numbers. Similar observations were also made by Dorsch, Krejsa, and Olsen (ref. 16) in their measurements of model blown-flap noise. In the discussion that follows, only the results for $M = 0.84$ are examined.

The sound field for the blown-flap noise is symmetrical only about the plane perpendicular to the wing-flap surface, which is the X-Y plane in figure 5. Therefore, the radiation characteristics of the sound are presented as a function of $\theta$ and $\phi$ defined in figure 5. Figure 11 illustrates the variation of OASPL with $\theta$ for three flap lengths in the planes corresponding to $\phi = 0^O$, $45^O$, and $90^O$. The OASPL variation in the plane perpendicular to the wing-flap surface and containing the jet axis ($\phi = 0^O$) is given in figure 11(a). Note that for the short flaps, the noise radiation exhibits a lobed pattern symmetrical about $\theta = 140^O$, which is approximately the mean direction of the flow leaving the trailing edge. The directional peak occurs in a direction nearly $30^O$ to the flow direction at the trailing edge ($110^O$ and $170^O$ from the inlet) as illustrated in figure 11(a). For the long flap $\left(l_f/d = 12.75\right)$, however, the directivity is unsymmetrical, and the OASPL below the wing (flow side, $\theta < 140^O$) is higher than that above the wing (no-flow side, $\theta > 140^O$). These results are not surprising, because the large surface (dimensions larger than the typical wavelength of the radiated sound) reflects the sound energy and thus provides shielding effects on the no-flow side of the surface.

The variation of OASPL in the plane corresponding to $\phi = 45^O$ is illustrated in figure 11(b). For $l_f/d = 3.75$, data were available only for $\theta = 200^O$ to $290^O$. The directivity pattern in this plane ($\phi = 45^O$) is not symmetrical with respect to the flap surface, because neither the geometry nor the flow is symmetrical in this plane. Note that the OASPL for the short flap generally exceeds that for the long flap at corresponding $\theta$ locations. Moreover, the OASPL for the short flap is higher on the no-flow side ($\theta > 140^O$) than on the flow side ($\theta < 140^O$).

Figure 11(c) illustrates the directional distribution of OASPL in the plane parallel to the wing surface and containing the jet axis ($\phi = 90^O$). The flow, the geometry, and thus the sound field are symmetrical about the jet axis in this plane; therefore, the radiated noise is measured only in one quadrant. The OASPL peaks at $\theta = 180^O$ (on the no-flow side of the flap) for the short flaps; for the long flap, the distribution appears to be nearly uniform. A dip in OASPL is also noted near $\theta = 110^O$ for $l_f/d = 0.75$ and 3.75.

10

Figure 12 illustrates the radiation characteristics of OASPL as a function of $\phi$ for three flap lengths in the planes corresponding to $\theta = 90^O$ (nozzle exit plane), $\theta = 130^O$, and $\theta = 160^O$. In the nozzle exit plane, the directional peak occurs at $\phi = 0^O$ (fig. 12(a)) directly below the wing (flow side). Also, the OASPL is not a minimum directly above the wing-flap ($\phi = 180^O$) except for $l_f/d = 12.75$. The directivity in the plane corresponding to $\theta = 130^O$ (fig. 12(b)) indicates that the values of OASPL are of the same order of magnitude both below and above the wing-flap for the short flaps. For the long flap, the OASPL below the wing is higher than above the wing. In the plane corresponding to $\theta = 160^O$ (fig. 12(c)), the variation of OASPL with $\phi$ is nearly uniform for a given flap length. The level, however, increases as the flap length is decreased.

The observed directivity pattern of the blown-flap noise is the result of three physical mechanisms: (1) the characteristics and location of the dominant source, (2) the acoustic refraction and scattering by the flow, and (3) the acoustic diffraction by the edges of the blown flap. The role that each mechanism plays in the observed directivity pattern is now examined. For the long flap, total power measurements indicate that the dominant source is the turbulent fluctuations due to flow impingement and the turbulent boundary layer on the flap surface. The interaction between turbulence and the trailing edge of the flap is only a secondary source. The dominant source is thus located on the flow side of the flap. The acoustic radiation observed on the no-flow side of the flap is the result of acoustic diffraction around the edges of the flap. Therefore, the OASPL should be considerably lower on the no-flow side than on the flow side. This is indeed the case. (See figs. 11(a), 11(b), 12(a), and 12(b).) For the short flaps, the total acoustic power varied with the fourth and fifth powers of jet velocity. From this observation, together with the existing theoretical analyses (refs. 14 and 15) on the possible mechanisms of blown-flap noise, it is reasonable to expect that the major noise source is the interaction between flow turbulence and flap trailing edge. If this is the case, the directivity pattern for the short flaps should be more or less symmetrical to the plane containing the trailing edge. (See fig. 11(a).) The refraction of sound by the asymmetric shear and shear gradient in the trailing-edge flow may play a role in changing the symmetry of the directivity pattern somewhat. However, since the extent of the trailing-edge flow in the direction perpendicular to the flap surface is small compared with the typical wavelength of radiated sound, the acoustic refraction by the flow is likely to be unimportant. Consequently, the observed directivity pattern for short flaps is governed mainly by the dominant source located around the flap trailing edge and by acoustic scattering of the sound generated by the flap surface.

Sound pressure level spectra.- The dependence of the spectral distribution of radiated noise on angular position of measurement is studied by examining the sound pressure

spectra at selected points in the plane perpendicular to the wing-flap surface and containing the jet axis. For the short flaps, the OASPL in this plane is nearly symmetrical about the flap angle ($\theta$ = 140°). Thus the sound pressure spectra obtained at four locations, two on the flow side ($\theta$ = 90° and 120°) and two on the no-flow side ($\theta$ = 170° and 230°), are examined in figure 13 as a function of flap length. The sound pressure spectra are normalized from 1/3-octave-band SPL with respect to individual bandwidths and OASPL. The peak frequencies below the wing (flow side) are generally higher than those above the wing (no-flow side). Compare figure 13(a) with 13(d) and compare figure 13(b) with 13(c). The spectrum for the shortest flap ($l_f/d$ = 0.75) in figure 13(a) indicates a possible screech at 2.5 kHz. In the high-frequency range, the spectra are similar for all flap lengths and fall off at a rate of 5 to 6 dB per octave. However, the radiated sound in the low-frequency range increases with flap length. A low-frequency hump around 200 Hz may also be noted for certain values of flap length at $\theta$ = 90°, 120°, and 230°. The spectral distribution of noise on the no-flow side of the wing (figs. 13(c) and 13(d)) indicates that for the long flap ($l_f/d$ = 12.75), most acoustic radiation is distributed below 300 Hz. For this flap length, noise is generated primarily by the turbulent flow over the wing-flap surface and is diffracted around the edges of the wing-flap.

## CONCLUSIONS

A simplified experimental model is used to investigate the acoustic characteristics and source mechanisms of an externally blown flap for STOL aircraft. The experimental results for total radiated acoustic power, directivity, sound power spectra, and sound pressure spectra are presented. The test parameters are flap length and jet Mach number. The following conclusions may be drawn from this investigation.

The radiated acoustic power of a jet impinging on a long flap, for which the flow velocity leaving the flap trailing edge is small, depends on the jet velocity raised to the eighth power, similar to free jet mixing. However, the acoustic power is increased above the free jet mixing noise by about 5 dB, most of the increase being in the low-frequency range. The noise propagates primarily on the flow side of the flap at an angle nearly 30° to the flow direction at the trailing edge. It may be conjectured that the major source mechanism is the Reynolds fluctuating stresses similar to those in a free jet but modified by the presence of the surface.

The acoustic power generated by the jet impinging on a short flap depends on the jet velocity raised to a power between four and five. A substantial part of the additional noise is generated in the low to intermediate frequencies, and the peak frequency

decreases as the flap length is increased. The directivity pattern of noise for a short flap is nearly symmetrical with respect to the flap trailing edge. The dominant source mechanism appears to be the interaction between the flow turbulence and the flap trailing edge.

Langley Research Center,
    National Aeronautics and Space Administration,
        Hampton, Va., April 16, 1975.

APPENDIX

THEORETICAL BACKGROUND

Theoretical developments concerning blown-flap noise are rather limited in extent. The available theories relevant to blown-flap noise are too sketchy to provide a full understanding of the mechanisms of noise generation and propagation. The theories of aerodynamic noise related to the externally blown flap are reviewed herein.

Curle (ref. 9) extended Lighthill's theory of aerodynamic noise and formulated a solution for the sound field generated by turbulent flow in the presence of solid boundaries. He showed that the effect of rigid boundary surfaces in the turbulent medium is equivalent to a distribution of dipoles, each representing the force with which a unit area of solid boundary acts upon the fluid. He derived the intensity of sound generated by quadrupoles $I_q$ and dipoles $I_d$ to be

$$I_q \propto \frac{\rho_o U_o^8 L^2}{c_o^5 R^2} f\left(N_{Re}\right)$$

$$I_d \propto \frac{\rho_o U_o^6 L^2}{c_o^3 R^2} g\left(N_{Re}\right)$$

where

L                           length scale

$N_{Re}$                   Reynolds number defined by $U_o$ and L

$f\left(N_{Re}\right), g\left(N_{Re}\right)$     functions of Reynolds number

As is evident from these expressions, at low Mach numbers the dipoles are more efficient radiators of sound than the quadrupoles. However, this formulation is applicable only to noise produced by bodies of small characteristic length compared with the wavelength of sound, such as a small airfoil in a turbulent airstream.

Phillips (ref. 10) considered the radiation of sound generated by the turbulent boundary layer on infinite and semi-infinite flat plates. For a fully developed boundary layer on an infinite surface, where the turbulence is homogeneous in the planes parallel to the surface and the flow is incompressible, he showed that the dipole sound energy radiation per unit area is zero. Therefore, in these regions, the noise is generated primarily

from the volume distribution of the quadrupoles. However, when the turbulence is not homogeneous in the planes parallel to the surface (such as near the leading and trailing edges and on curved surfaces), the dipole sound radiation is not zero.

Powell (ref. 11) considered the noise generated by aerodynamic instabilities in the presence of a plane boundary. The image principle is developed to show that the pressures exerted on a plane boundary are reflections of the quadrupole generators of the flow itself. For sound with large wavelengths, the quadrupole sound intensity is enhanced. Therefore, he argued that the surfaces have a purely passive role in noise generation and radiation. The plane in the turbulence enhances the sound intensity for the quadrupole generators close to the plane by a factor of 4 above the sound that would be radiated into the half-space in the hypothetical absence of the plane. Therefore, the dimensional dependence of the acoustic power should be similar to that of unbound volume distribution of aerodynamic stress sources.

In reference 13, Meecham included the effect of curvature of a rigid boundary on aerodynamic sound generation. Using the image argument, he deduced the following expression:

$$\text{(Actual flow)} - \text{(Image flow)} \propto \left(\frac{\delta}{r_c}\right) \text{(Image flow)}$$

where $\delta$ is the boundary-layer thickness and $r_c$ is the radius of curvature. The ratio between the dipole surface sound $I_d$ and quadrupole volume sound $I_q$ is given by

$$\frac{I_d}{I_q} \propto \frac{K_d}{K_q}\left(\frac{c_o}{U_o}\right)^2\left(\frac{\delta}{r_c}\right)^2$$

where $K_d$ and $K_q$ are constants and in general, the ratio of these constants is very small $\left(\text{of the order of } 2 \times 10^{-5}\right)$. Therefore, for an object with large radius of curvature compared with the boundary-layer thickness, the dipole sound is greatly reduced at high subsonic Mach numbers. Meecham argues that, even though the wavelength has to be taken into account, the influence of wavelength on reflection and diffraction does not appreciably change the total sound radiated for rigid surfaces. Therefore, he concludes that because of the enhancement of the quadrupole sound by the shear flow effects in the boundary layer and because of the effect of small curvature which further reduces the amount of the dipole sound by a factor of $\left(\delta/r_c\right)^2$, volume quadrupole sound is dominant over surface dipole sound for slightly curved smooth surfaces.

Powell (ref. 12) investigated the radiated sound from a finite, rigid, flat plate moving at zero incidence. He conjectured that there are three primary sources of sound generation: (1) layer noise, (2) edge noise, and (3) wake noise. A layer noise (quadrupole

noise) arises from the volume of turbulence adjacent to the plate. Using the image argument, he concluded that the pressure fluctuations between the fluid and the plate are ineffective in generating the acoustic energy to radiate. However, near the edges of the finite plate, the pressure dipole radiation may generate from strips adjacent to the edges. According to a dimensional analysis, this edge noise should depend on the sixth power of mean velocity. However, since the effective width of the strips along the edges increases with the distance from the leading edge and decreases with the flow velocity, the radiated acoustic power depends on the velocity raised to between the fourth and fifth powers.

Ffowcs Williams and Hall (ref. 14) studied the effect of fluctuating turbulent stresses near the scattering edge of a semi-infinite rigid plane. They considered the basic Lighthill equation for aerodynamic noise generation and propagation in the presence of a rigid half-plane and formulated an integral solution in terms of an appropriate Green function. For eddies near the edge ($2kr \ll 1$), they obtained the far-field sound intensities in terms of $(2kr)^{-3/2}$, $(2kr)^{-1/2}$, and positive powers of $(2kr)$, where $k$ is the wave number and $r$ is the distance from the center of the turbulence volume. Since $2kr \ll 1$, the terms containing $(2kr)^{-3/2}$ are dominant. Considering only the dominant terms, the far-field sound intensity of quadrupole sources near the edge is given by

$$I_q = \frac{k^4 \rho_o U_o^4 \alpha^2}{c_o R^2 (kr)^3} V^2 f$$

where

$\alpha$          ratio of fluctuating velocity to typical velocity

$V$          volume of eddies

$f$          directivity function

The frequency of the turbulence source is of the order of $U_o/2\delta$ and $k = \pi U_o/c_o \delta$, where $2\delta$ is the extent of the turbulent region. Therefore, the scattered intensity increases in proportion to the fifth power of the typical fluid velocity.

Hayden (ref. 15) studied the radiated sound due to flow on a flat plate leaving the trailing edge. His theoretical model consists of dipole sources generated at the trailing edge by imparting the fluctuating momentum to the unbounded free field, with preferred sources perpendicular to the plate. After modifying the solution to account for the boundary condition of zero normal velocity on the rigid surface, he derived a sixth-power velocity dependence for the radiated sound intensity. The directivity is given as proportional to $\cos^2 \frac{\theta}{2}$, where $\theta$ is defined in figure 5.

16

# REFERENCES

1. Hubbard, Harvey H.; Chestnutt, David; and Maglieri, Domenic J.: Noise Control Technology for Jet-Powered STOL Vehicles. ICAS Paper No. 72-50, Aug.-Sept. 1972.

2. Olsen, William A.; Miles, Jeffrey H.; and Dorsch, Robert G.: Noise Generated by Impingement of a Jet Upon a Large Flat Board. NASA TN D-7075, 1972.

3. Olsen, William A.; Dorsch, Robert G.; and Miles, Jeffrey H.: Noise Produced by a Small-Scale Externally Blown Flap. NASA TN D-6636, 1972.

4. Gibson, Frederick W.: Noise Measurements of Model Jet-Augmented Lift Systems. NASA TN D-6710, 1972.

5. Kantarges, George T.; and Cawthorn, Jimmy M.: Effects of Temperature on Noise of Bypass Jets as Measured in the Langley Noise Research Facility. NASA TN D-2378, 1964.

6. Gruschka, Heinz D.; and Schrecker, Gunter O.: Aeroacoustic Characteristics of Jet Flap Type Exhausts. AIAA Paper No. 72-130, Jan. 1972.

7. Strong, D. R.; Siddon, T. E.; and Chu, W. T.: Pressure Fluctuations on a Flat Plate With Oblique Jet Impingement. NASA CR-839, 1967.

8. Westley, R.; Woolley, J. H.; and Brosseau, P.: Surface Pressure Fluctuations From Jet Impingement on an Inclined Flat Plate. Symposium on Acoustic Fatigue, AGARD-CP-113, May 1973, pp. 4-1 — 4-17.

9. Curle, N.: The Influence of Solid Boundaries Upon Aerodynamic Sound. Proc. Roy. Soc. (London), ser. A, vol. 231, no. 1187, Sept. 20, 1955, pp. 505-514.

10. Phillips, O. M.: On the Aerodynamic Surface Sound From a Plane Turbulent Boundary Layer. Proc. Roy. Soc., ser. A, vol. 234, no. 1198, Feb. 21, 1956, pp. 327-335.

11. Powell, Alan: Aerodynamic Noise and the Plane Boundary. J. Acoust. Soc. Amer., vol. 32, no. 8, Aug. 1960, pp. 982-990.

12. Powell, Alan: On the Aerodynamic Noise of a Rigid Flat Plate Moving at Zero Incidence. J. Acoust. Soc. Amer., vol. 31, no. 12, Dec. 1959, pp. 1649-1653.

13. Meecham, William C.: Surface and Volume Sound From Boundary Layers. J. Acoust. Soc. Amer., vol. 37, no. 3, Mar. 1965, pp. 516-522.

14. Ffowcs Williams, J. E.; and Hall, L. H.: Aerodynamic Sound Generation by Turbulent Flow in the Vicinity of a Scattering Half Plane. J. Fluid Mech., vol. 40, pt. 4, Mar. 1970, pp. 657-670.

15. Hayden, Richard E.: Noise From Interaction of Flow With Rigid Surfaces: A Review of Current Status of Prediction Techniques.  NASA CR-2126, 1972.

16. Dorsch, Robert G.; Krejsa, Eugene A.; and Olsen, William A.:  Blown Flap Noise Research.  AIAA Paper No. 71-745, June 1971.

$l$ = 17.1 cm (6.75 in.)
d = 5.1 cm (2 in.)
$r_c$ = 40.6 cm (16 in.)
x = 29.2 cm (11.5 in.)
y = 10.2 cm (4 in.)
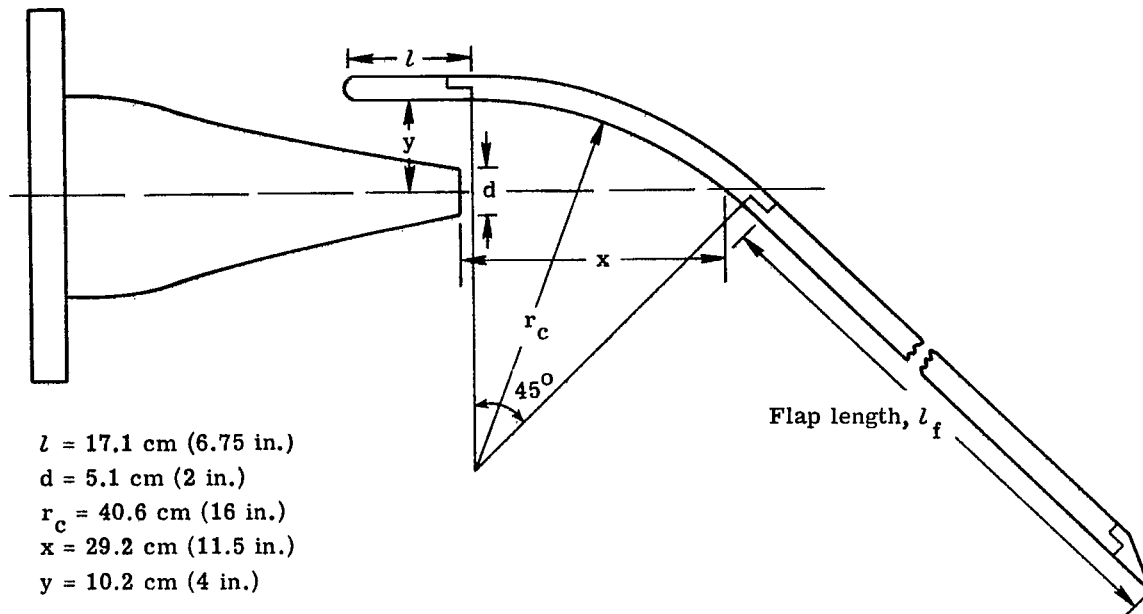
Figure 1.- Schematic sketch of blown-flap model.
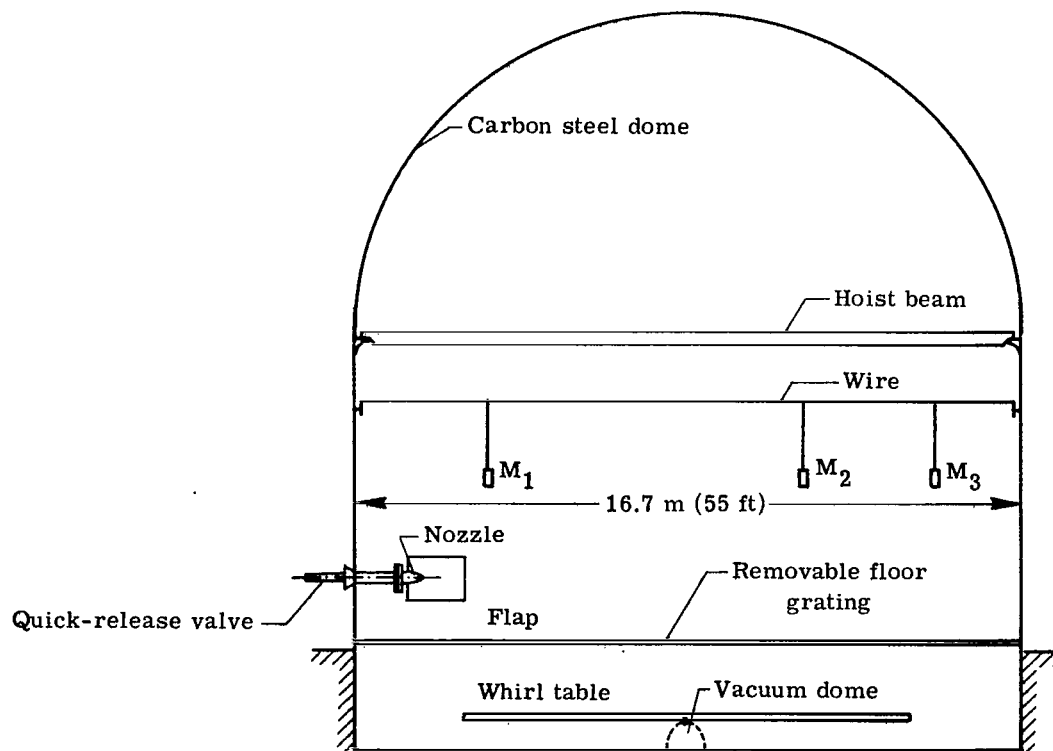


Figure 2.- Blowdown jet and reverberation chamber with experimental setup. Chamber volume, 2830 m$^3$ (10$^5$ ft$^3$). $M_1$, $M_2$, and $M_3$ are microphones.
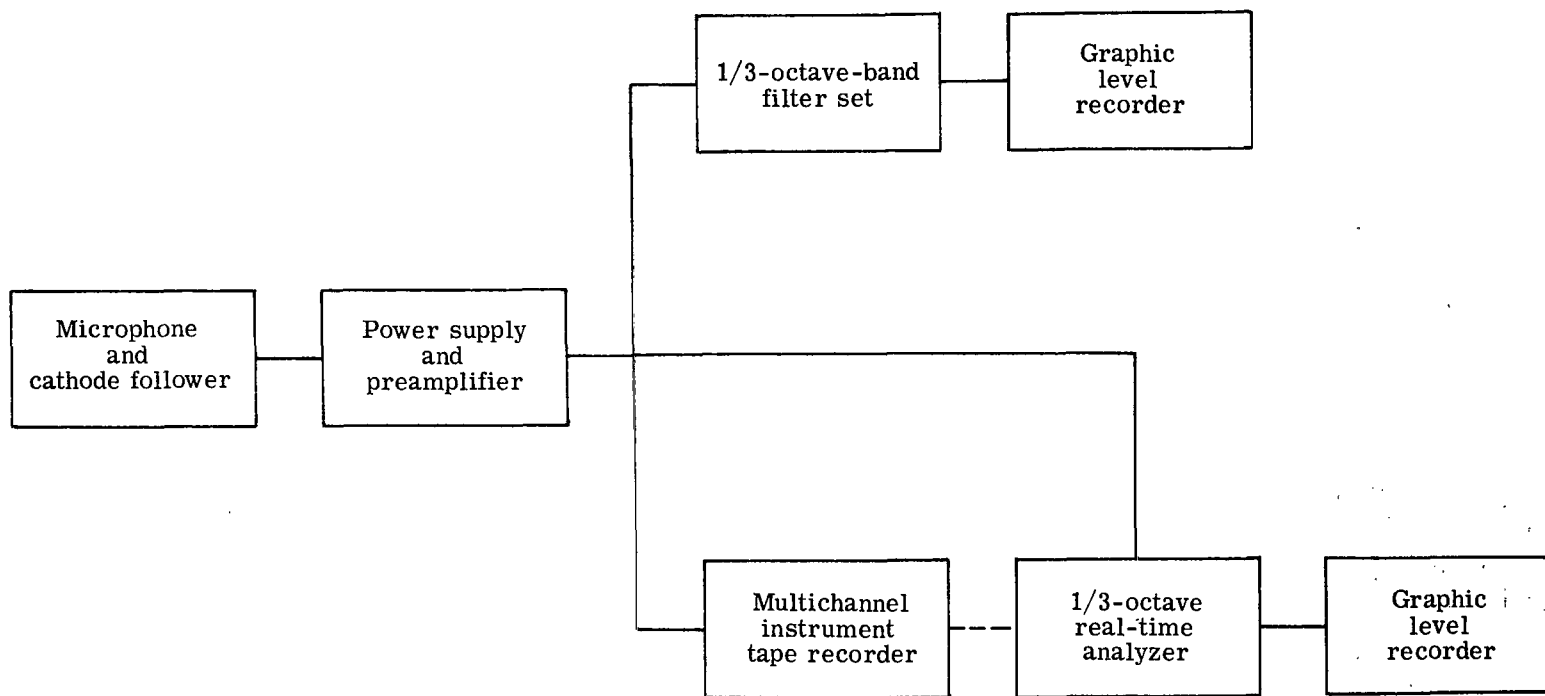
Figure 3.- Block diagram showing acoustic instrumentation.
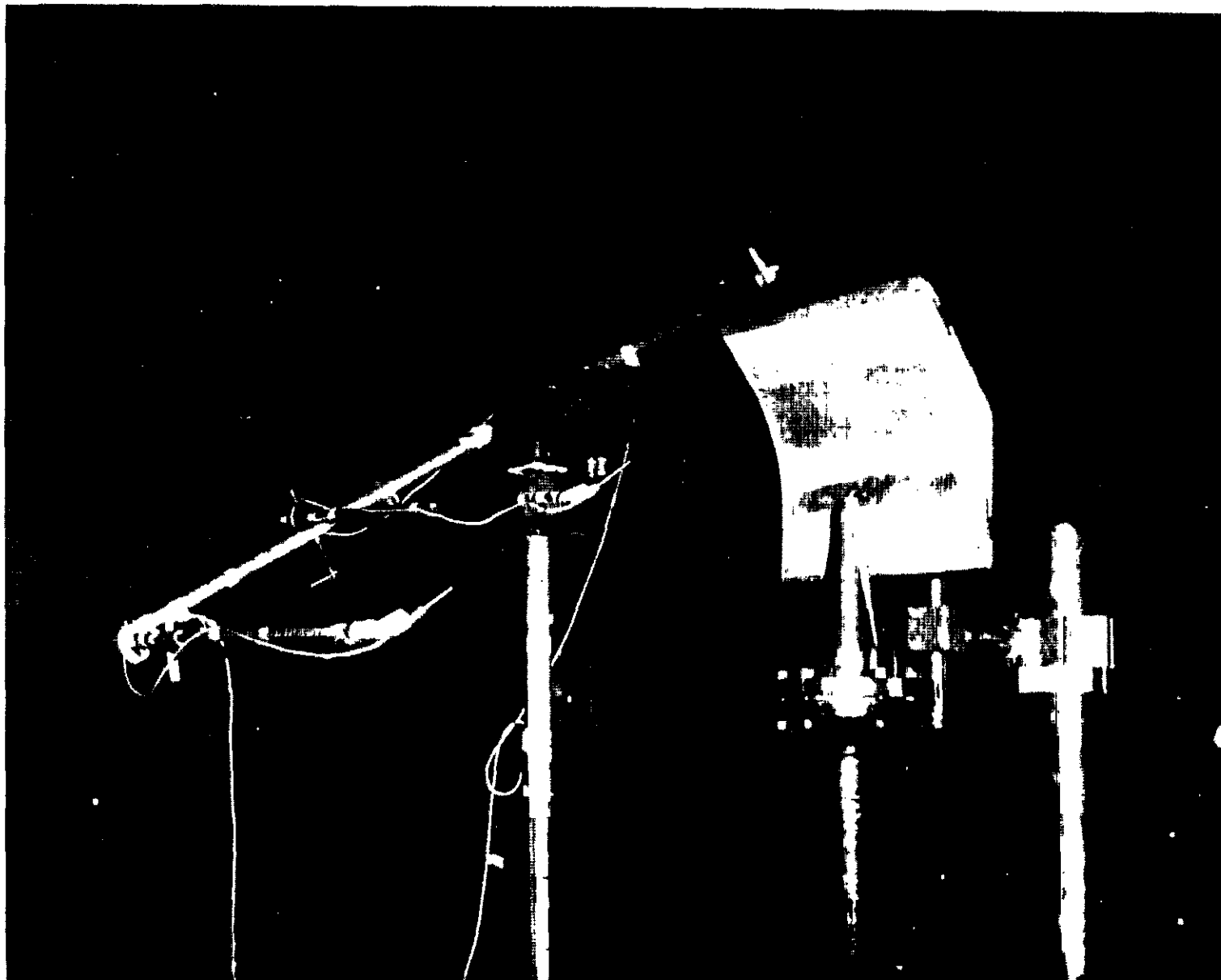
Figure 4.- Experimental model in anechoic chamber.

L-73-2412
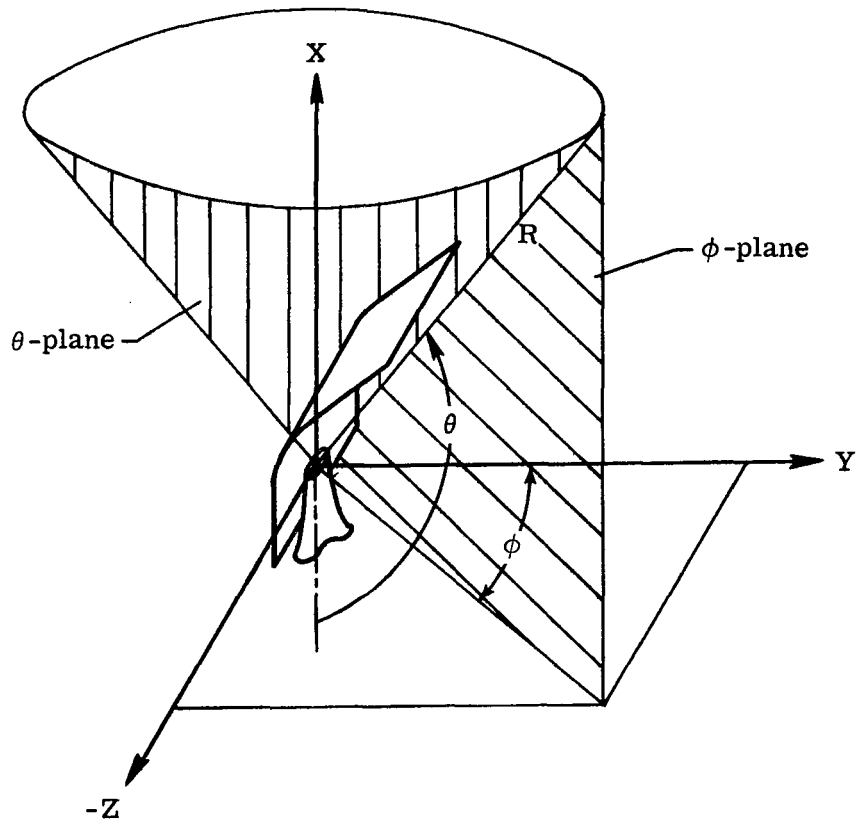
Figure 5.- Sketch showing coordinate system used
in directivity measurements.
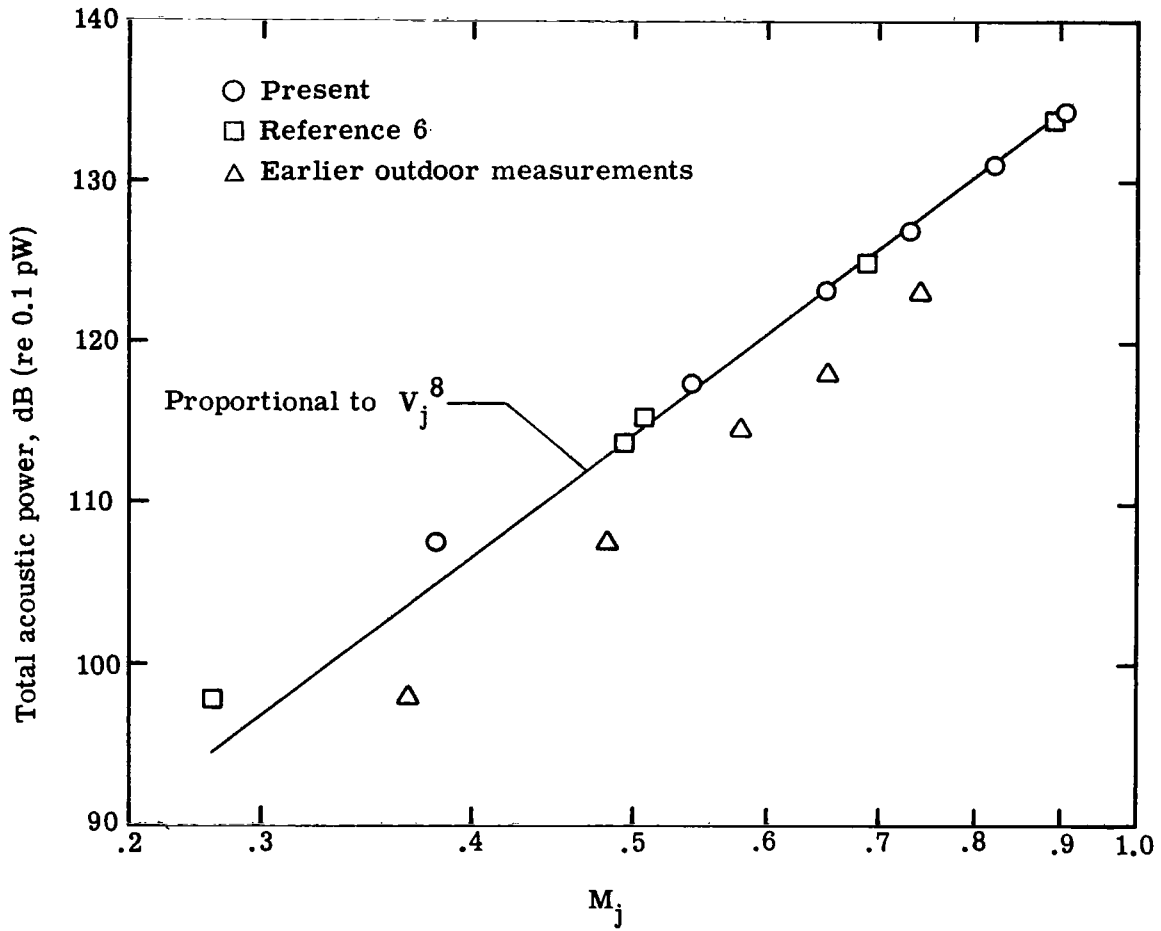
Figure 6.- Total acoustic power variation with jet Mach number for free jet mixing.
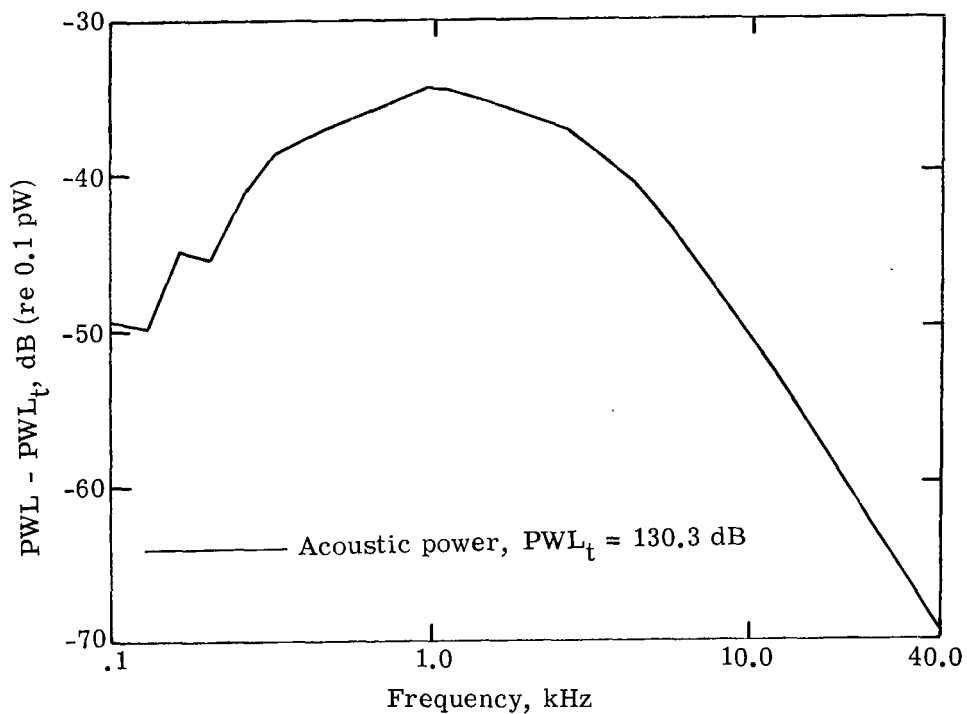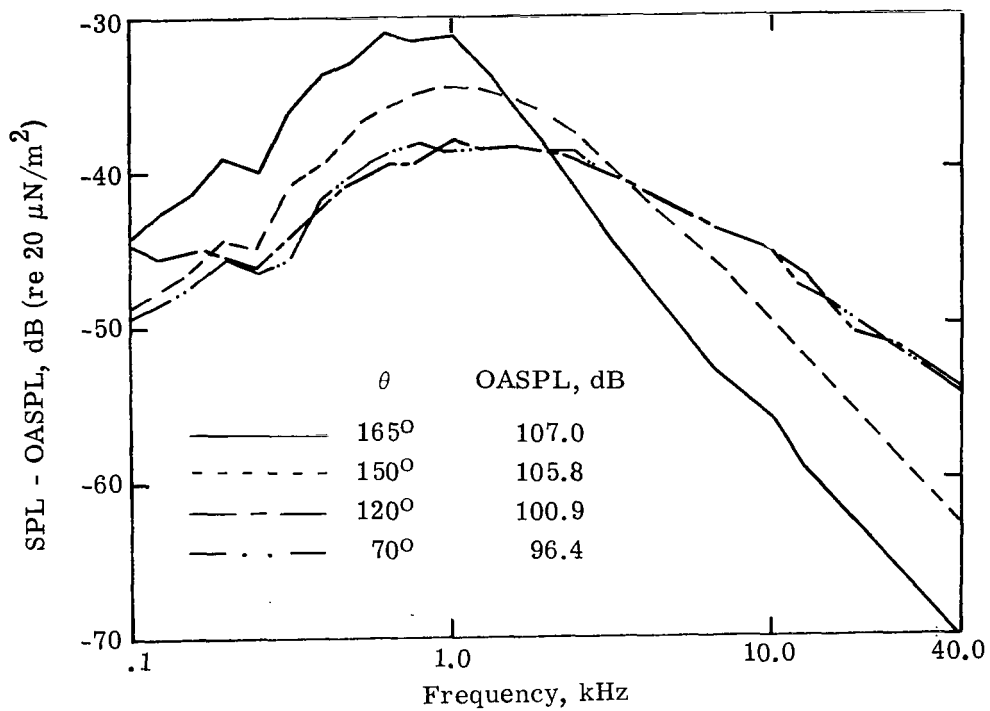
Figure 7.- Spectral variation of jet mixing noise with angle from jet intake.
Jet alone; $M_j = 0.85$.
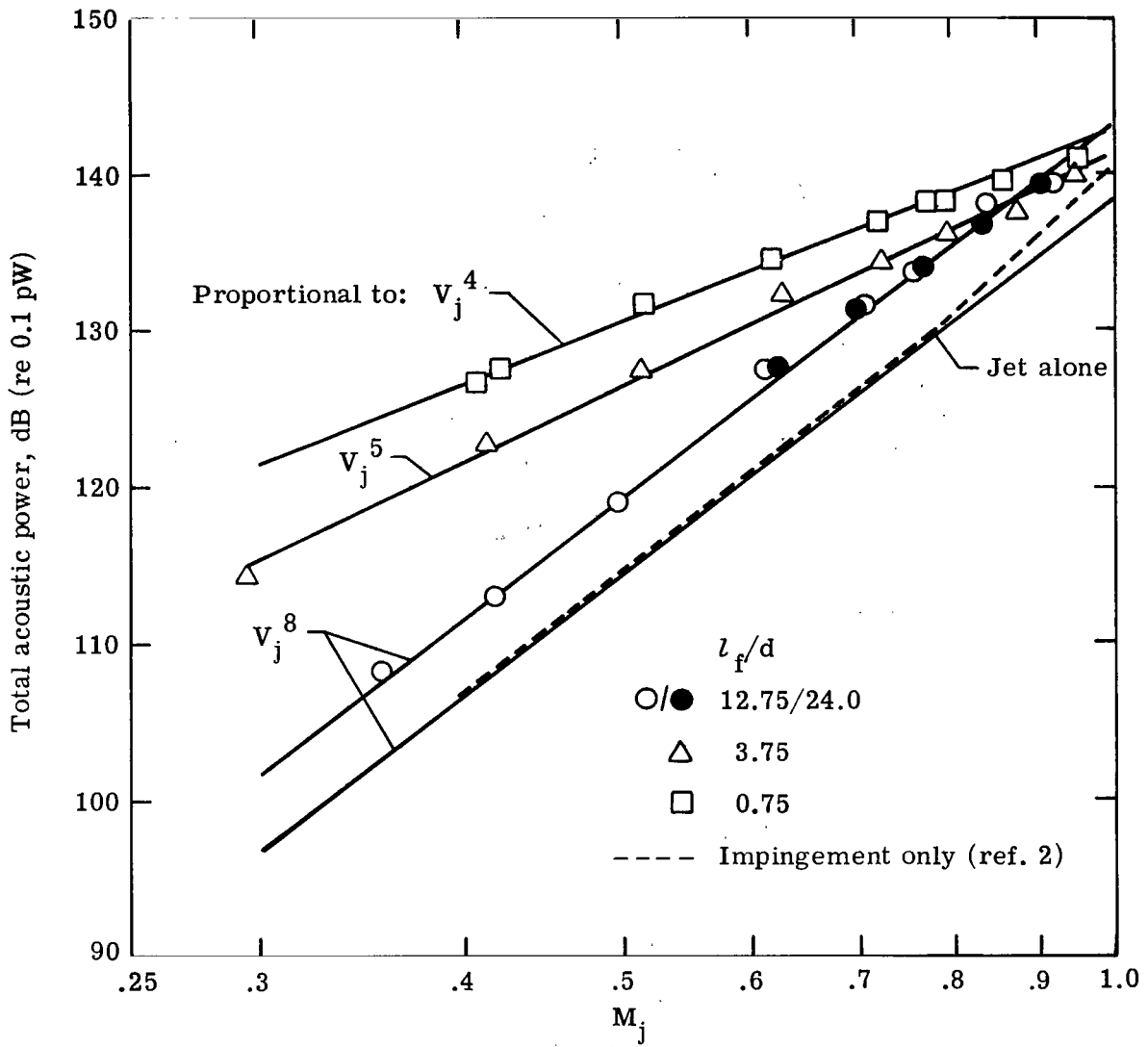
Figure 8.- Variation of total acoustic power radiated by blown flap with jet Mach number.
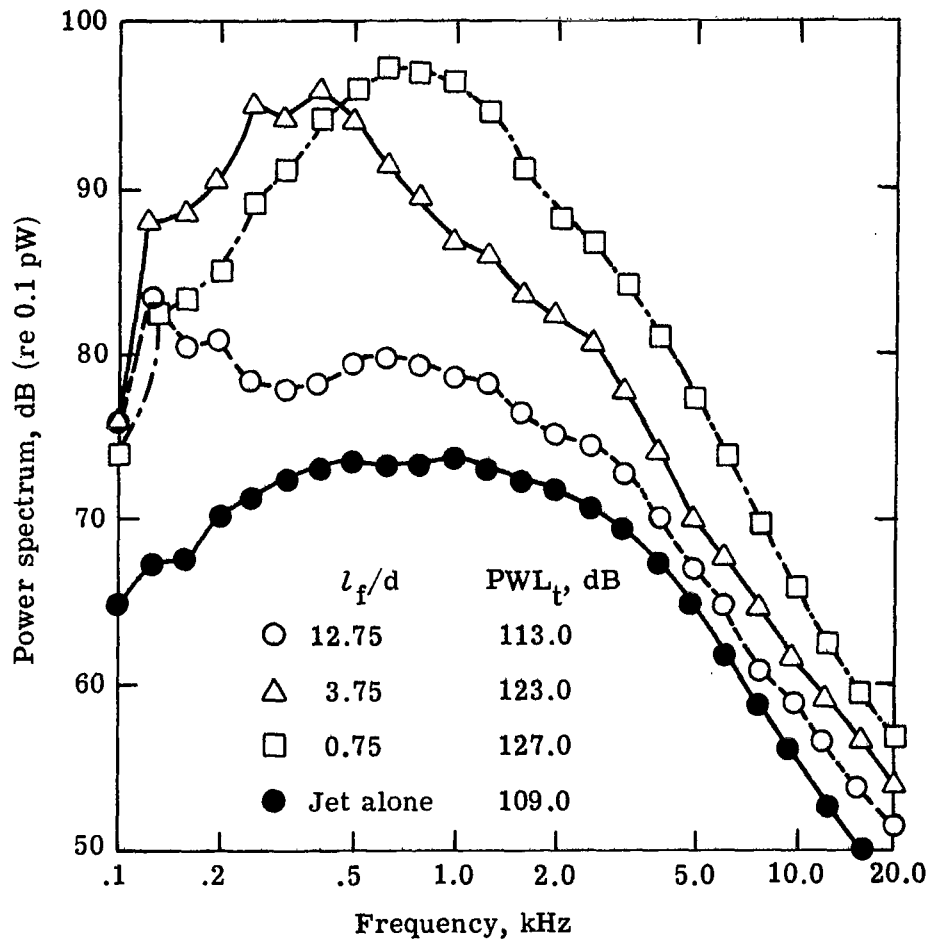
(a)  $M_j = 0.42$.

Figure 9.- Effect of flap length on sound power spectra.
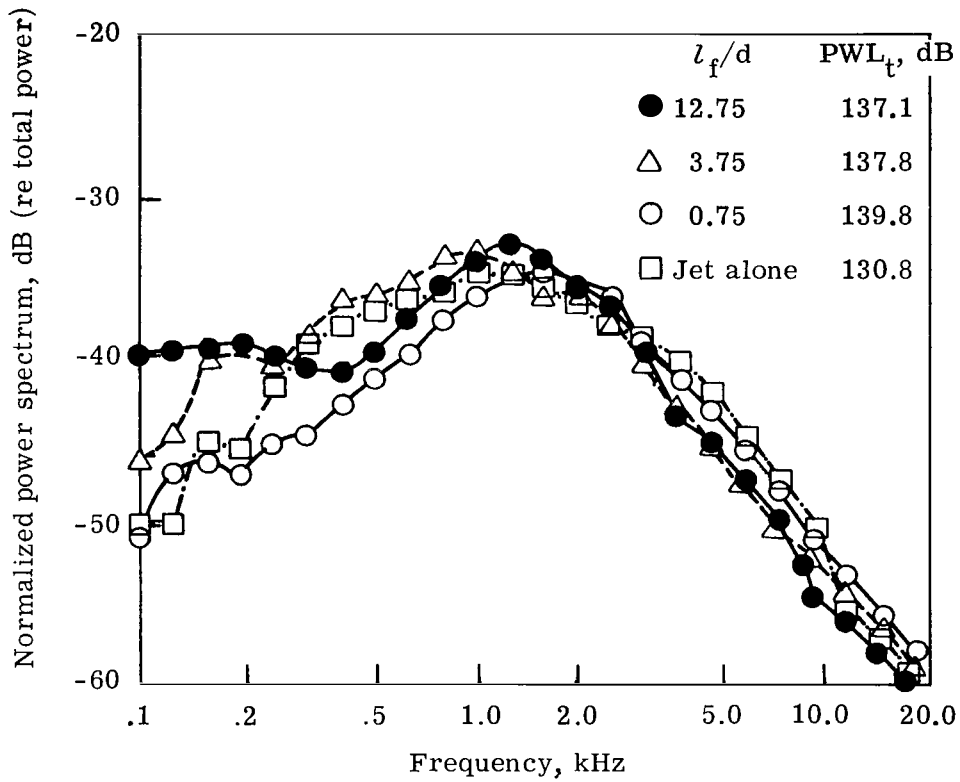
(b)   $M_j = 0.83$.

Figure 9.- Concluded.
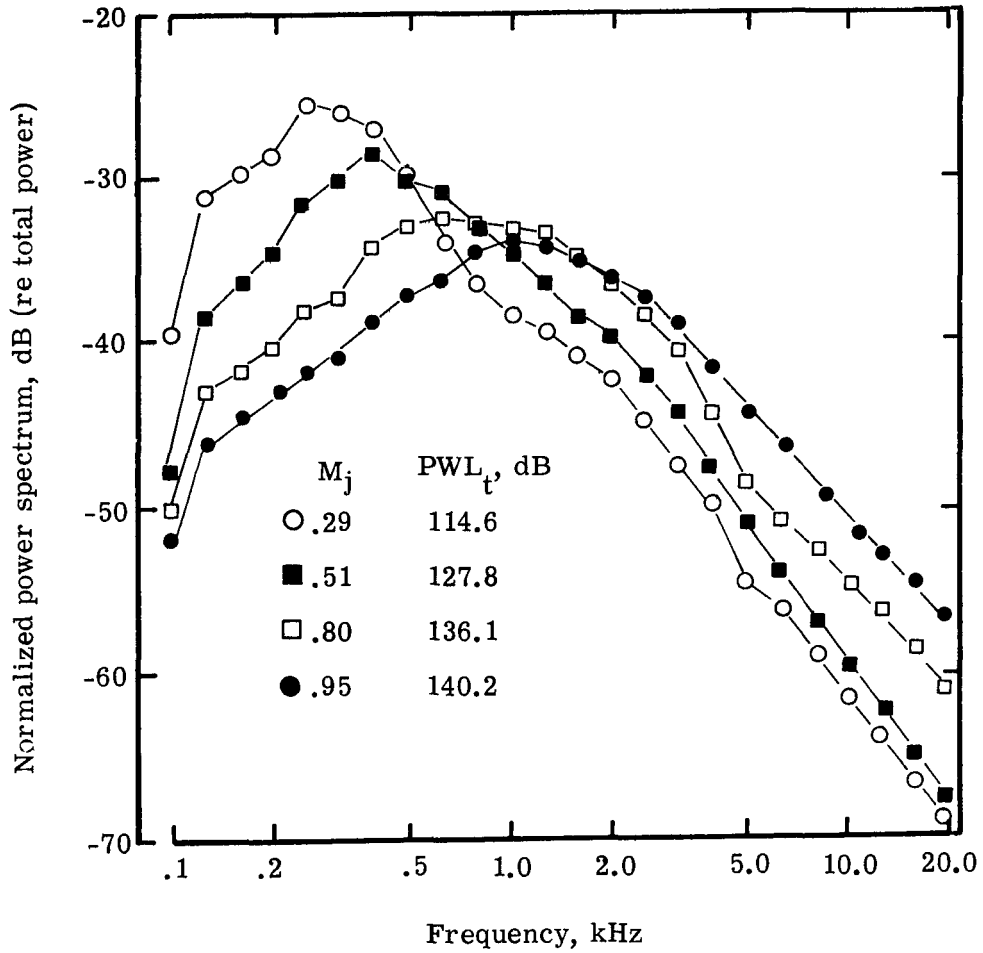
Figure 10.- Power spectra variation with jet Mach number. $l_f/d = 3.75$.
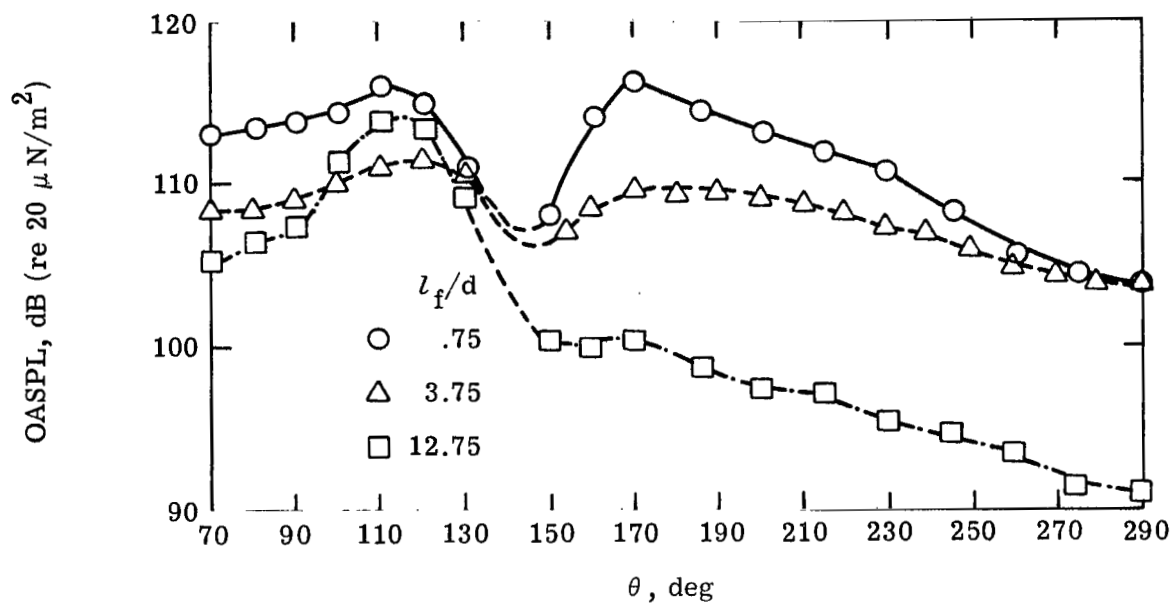
(a)  $\phi = 0^{\circ}$.
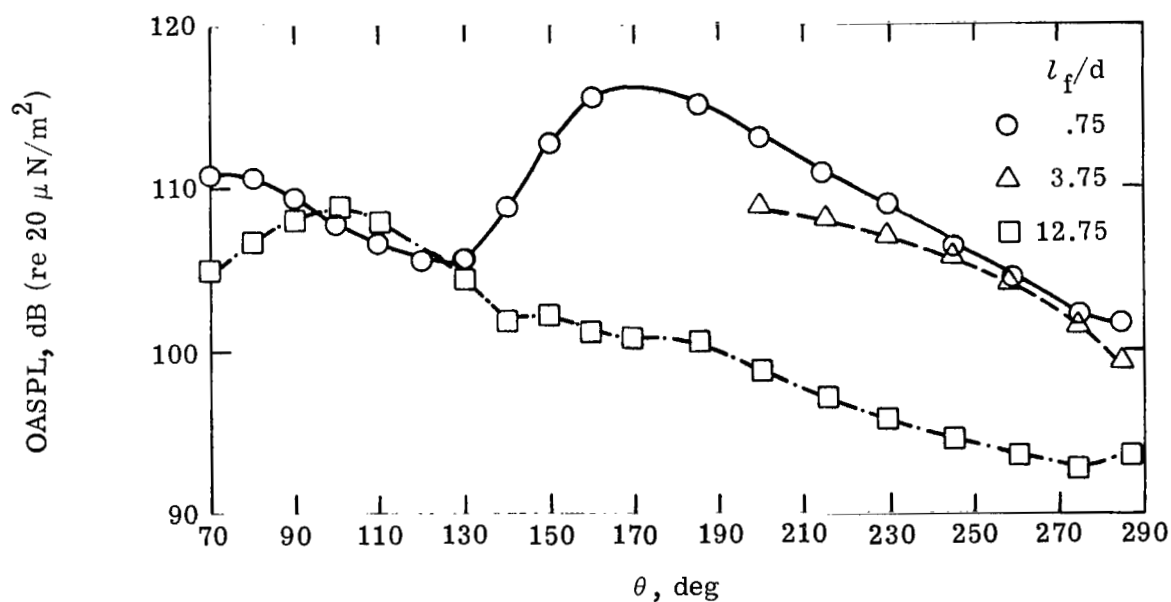


(b)  $\phi = 45^{\circ}$.

Figure 11.- Directivity pattern of OASPL for various flap lengths as a function of  $\theta$.
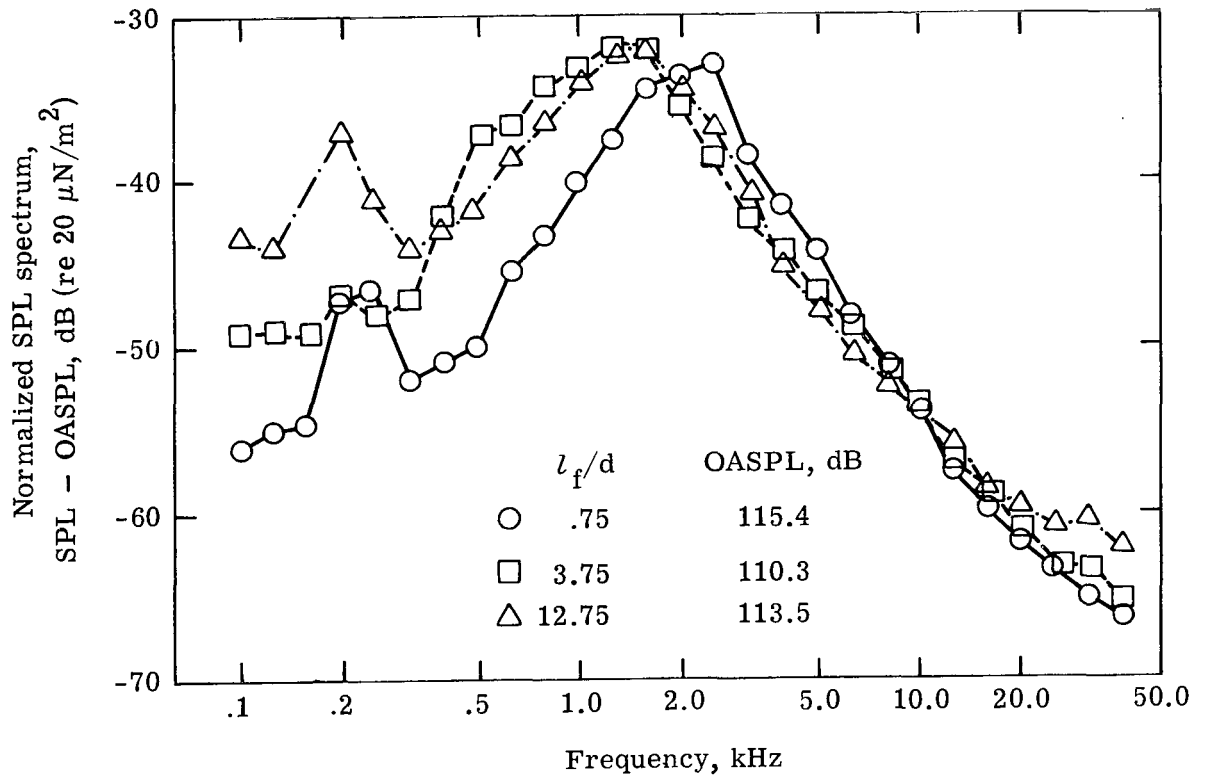$M_j = 0.84$.

Axis of symmetry
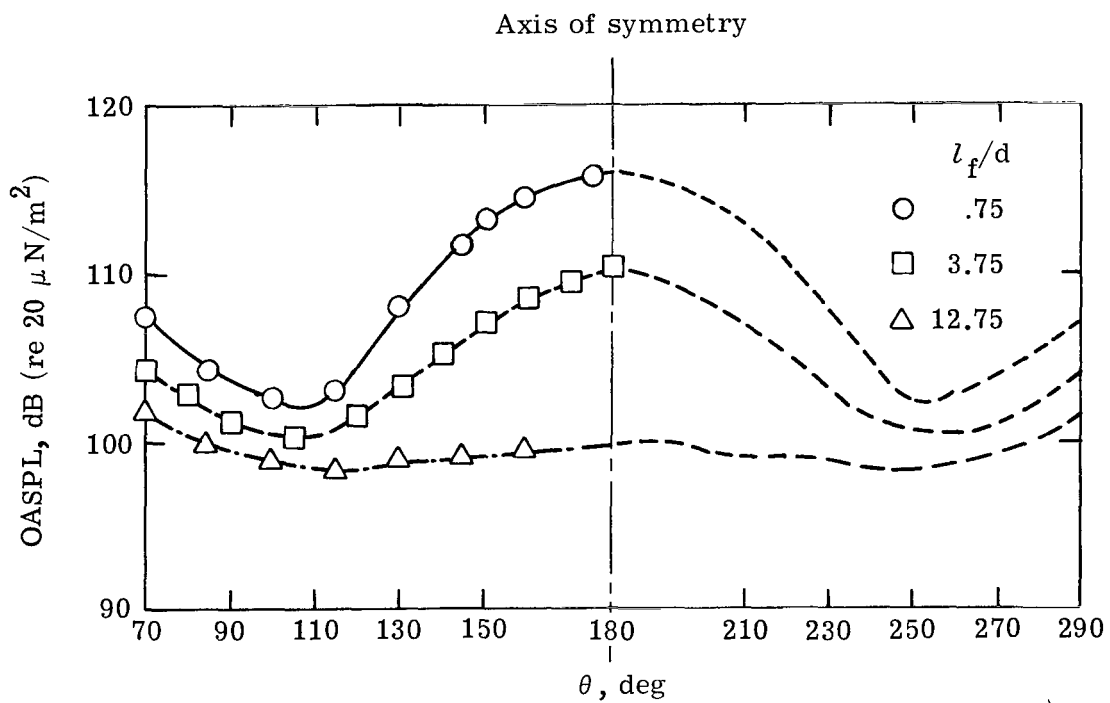


(c)  $\phi = 90^{\circ}$.

Figure 11.- Concluded.

(a) $\theta = 90^O$.



(b) $\theta = 130^O$.
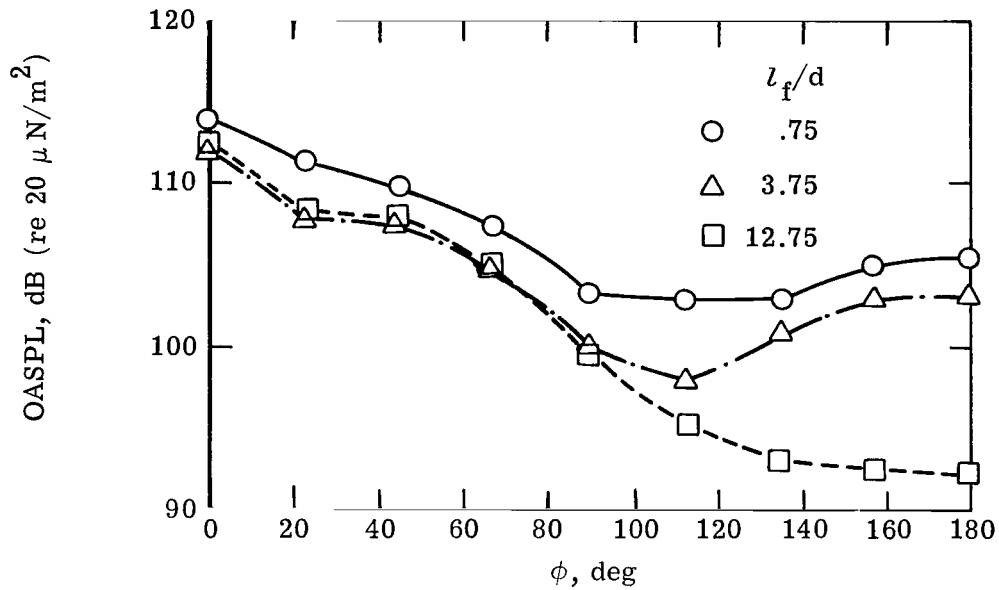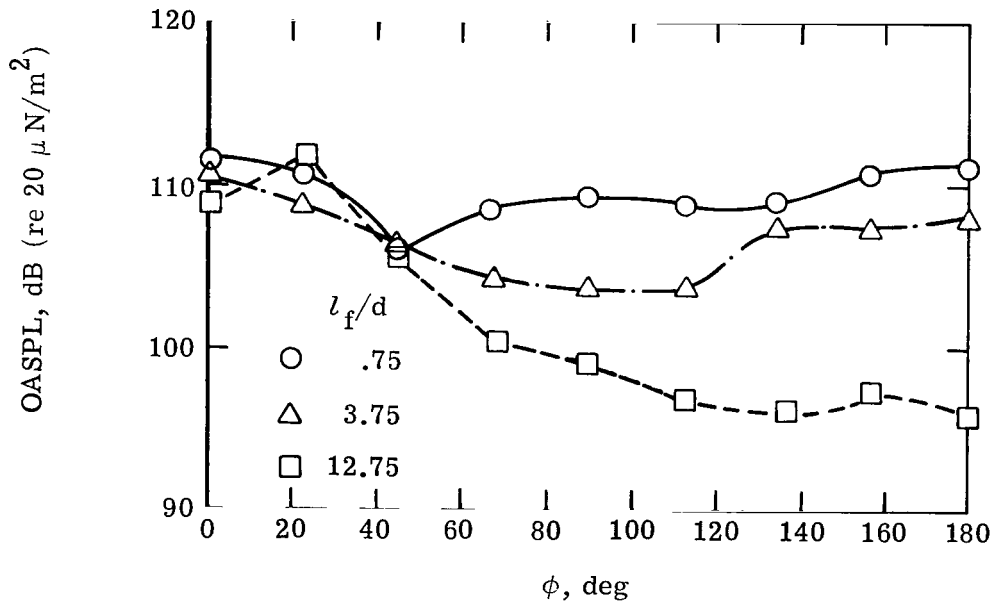
Figure 12.- Directivity pattern of OASPL for various flap lengths as a function of $\phi$. $M_j = 0.84$.

(c)  $\theta = 160^{\text{O}}$.
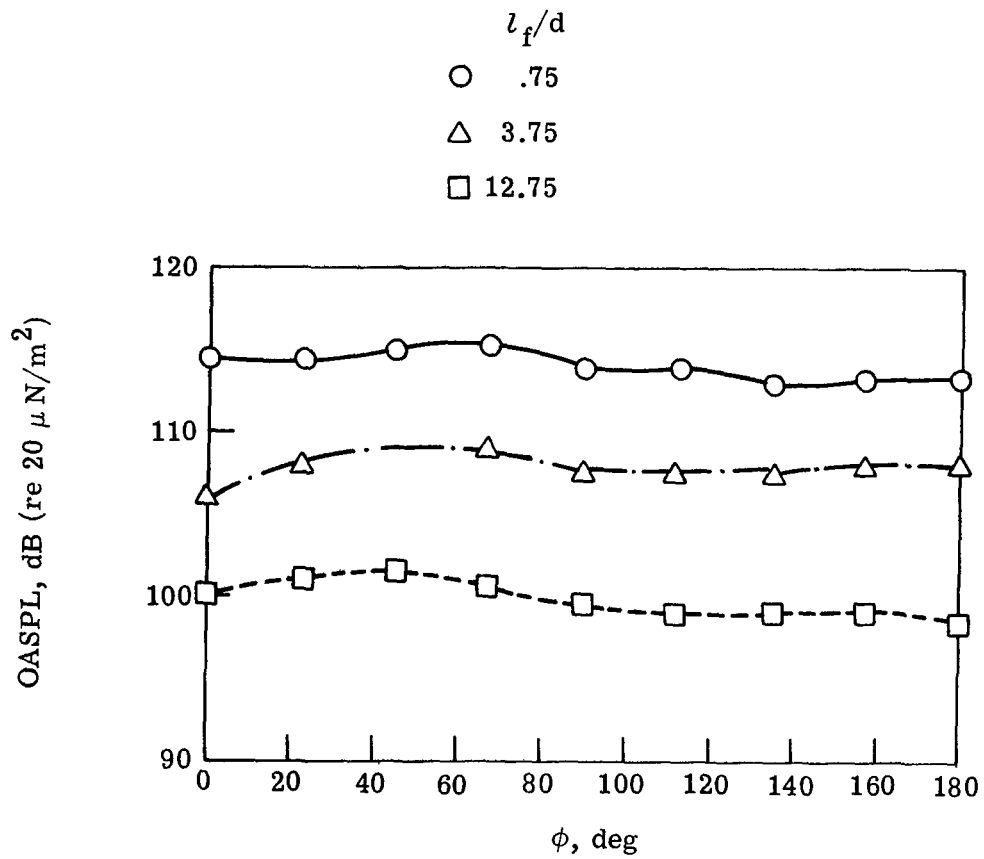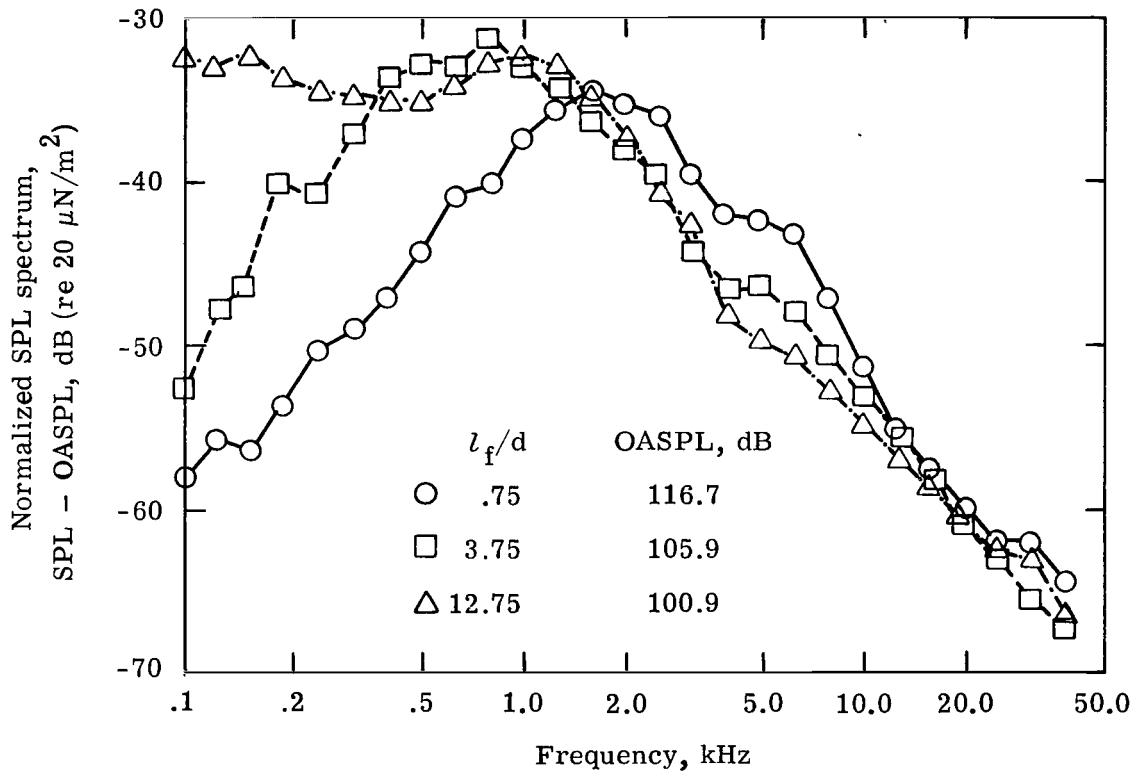
Figure 12.- Concluded.
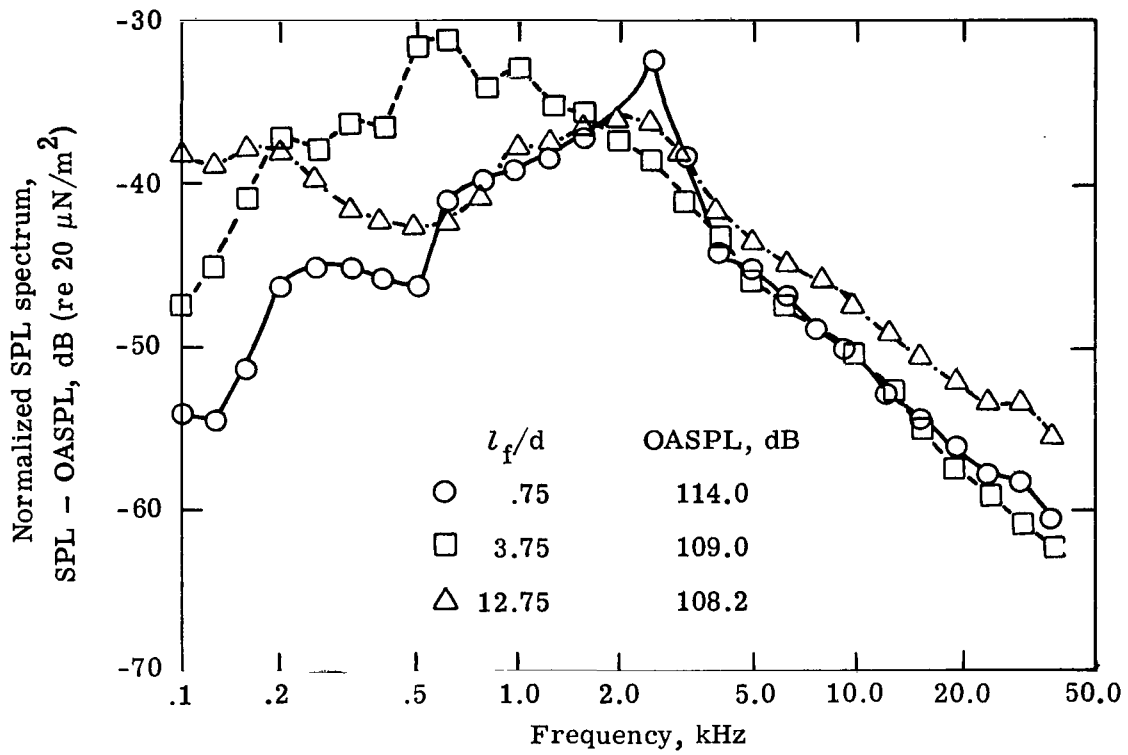
(a)  $\theta = 90^{\circ}$.

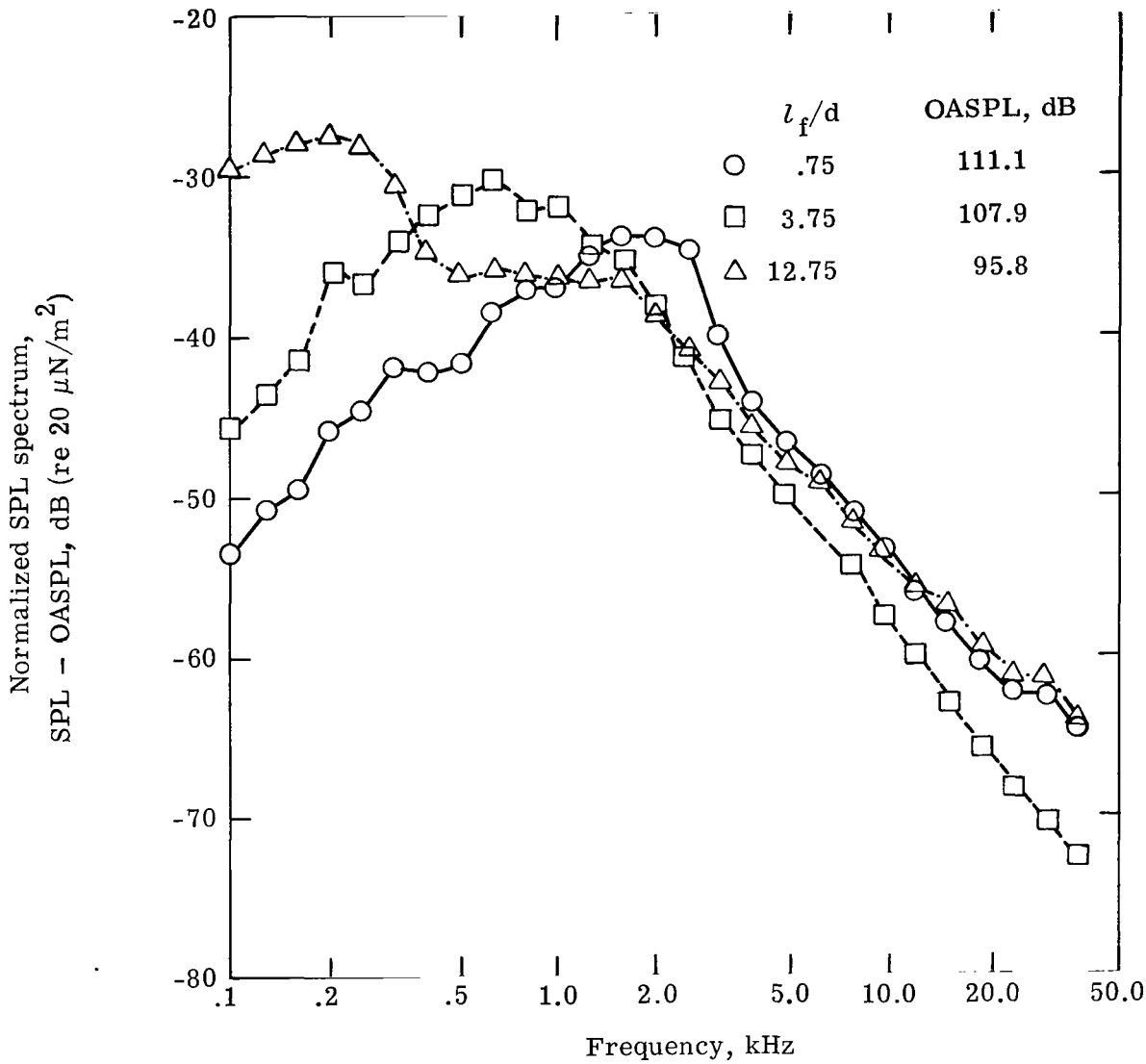Figure 13.- Sound pressure level spectra.  M = 0.84;  $\phi = 0^{\circ}$.

(b) $\theta = 120^{\circ}$.

Figure 13.- Continued.

(c)  $\theta = 170^O$.

Figure 13.- Continued.

(d)  $\theta = 230^{\circ}$.

Figure 13.- Concluded.

*"The aeronautical and space activities of the United States shall be conducted so as to contribute . . . to the expansion of human knowledge of phenomena in the atmosphere and space. The Administration shall provide for the widest practicable and appropriate dissemination of information concerning its activities and the results thereof."*
—NATIONAL AERONAUTICS AND SPACE ACT OF 1958

# NASA SCIENTIFIC AND TECHNICAL PUBLICATIONS

TECHNICAL REPORTS: Scientific and technical information considered important, complete, and a lasting contribution to existing knowledge.

TECHNICAL NOTES: Information less broad in scope but nevertheless of importance as a contribution to existing knowledge.

TECHNICAL MEMORANDUMS: Information receiving limited distribution because of preliminary data, security classification, or other reasons. Also includes conference proceedings with either limited or unlimited distribution.

CONTRACTOR REPORTS: Scientific and technical information generated under a NASA contract or grant and considered an important contribution to existing knowledge.

TECHNICAL TRANSLATIONS: Information published in a foreign language considered to merit NASA distribution in English.

SPECIAL PUBLICATIONS: Information derived from or of value to NASA activities. Publications include final reports of major projects, monographs, data compilations, handbooks, sourcebooks, and special bibliographies.

TECHNOLOGY UTILIZATION PUBLICATIONS: Information on technology used by NASA that may be of particular interest in commercial and other non-aerospace applications. Publications include Tech Briefs, Technology Utilization Reports and Technology Surveys.

*Details on the availability of these publications may be obtained from:*

**SCIENTIFIC AND TECHNICAL INFORMATION OFFICE**

**NATIONAL AERONAUTICS AND SPACE ADMINISTRATION**

**Washington, D.C. 20546**